

Electron-Electron Interactions in Expanded-Metal Compounds*

ANGELICA M. STACY,[†] PETER P. EDWARDS,[‡] AND M. J. SIENKO[§]

Baker Laboratory of Chemistry, Cornell University, Ithaca, New York 14853

Received April 29, 1982

Magnetic studies by the Faraday method were carried out over the range 4.2–200K on a variety of structures in which lithium metal was progressively "expanded." At one extreme is tetrakisammonia-lithium(zer0), $\text{Li}(\text{NH}_3)_4$, which is Pauli metallic; at the other is monolithium [2.1.1] cryptate electride, the magnetic behavior of which is clearly nonmetallic. Intermediate, apparently just on the nonmetallic side of the metal-nonmetal transition, is the solid tetrakisethylammoniumlithium(zer0), $\text{Li}(\text{C}_2\text{H}_5\text{NH}_2)_4$. The electronic behavior of these "expanded-metal" compounds is interpreted in terms of Hubbard bands and Mott-Anderson transitions. The dielectric constant of the host matrix is crucial for scaling the onset of metallic behavior.

Introduction

One of the most remarkable features of metal-ammonia systems is the deep eutectic that characterizes solidification of the saturated solutions (1). In the case of lithium-ammonia, considerable evidence has accumulated to the effect that a compound, $\text{Li}(\text{NH}_3)_4$, is formed in conjunction with this eutectic, although the precise phase relations around the eutectic point (89K, 20 mole% Li) are still in doubt (2). The electric and magnetic properties of $\text{Li}(\text{NH}_3)_4$ are highly unusual, suggesting that the compound, which can be thought of as lithium metal expanded by insertion of

ammonia, is just on the verge of a metal-nonmetal transition. The electrical resistivity (3) follows a T^2 law in the range 1.5–30K, a T law to 65K, then flattens out. At 82K, there is a solid-solid transition which is accompanied by a 20% drop in resistivity. At 89K, melting occurs with a sixfold increase in resistivity. The liquid shows decreasing resistance with increasing temperature. The magnetic susceptibility (4) of the liquid is temperature-independent at $+60 \times 10^{-6}$ emu/mole (after correction for core diamagnetism), which is consistent with a Pauli metal. Below the solidification point at 89K there is a small drop in χ but it essentially stays constant from 89 to 82K. At 82K, there is a 40% drop with onset of a temperature-dependent increase down to about ~ 25 K, below which χ decreases. Although the thermal variation of χ was recognized as being most unusual, not much quantitative significance was attached to the values, as it was extraordinarily difficult to determine absolute Faraday susceptibilities and to make precise corrections for the

* Presented at the Symposium on the Electronic Structure and Bonding in Solids, 183rd National Meeting, American Chemical Society, held in Las Vegas, Nevada, March 30–31, 1982.

[†] Present address: Department of Chemistry, Northwestern University, Evanston, Ill. 60201.

[‡] Present address: University Chemical Lab, Lensfield Road, Cambridge, CB2 1EW, United Kingdom.

[§] Author to whom correspondence should be addressed.

containers and core diamagnetism. Recently, in collaboration with Dye and Landers (5), we have made a precise study of the magnetic susceptibility of Li [2.1.1] cryptate electride in which we found it possible to correct directly for sample vial and diamagnetic cores by allowing the sample to decompose *in situ* and by remeasuring the residue in the intact container. By applying the same technique to $\text{Li}(\text{NH}_3)_4$, we have reproduced the results of Glaunsinger *et al.*, showing in particular that there is indeed a maximum in the solid susceptibility at about 25K with apparent antiferromagnetic ordering below this temperature (6).

Most of the data on $\text{Li}(\text{NH}_3)_4$ have been interpreted in terms of structural information obtained by powder X-ray diffraction studies of Mammano and Sienko (7). Believing that two solid phases were present at 77K, they suggested a cubic form with $a = 9.55 \text{ \AA}$ for solid phase I (stable between 82 and 89K) and a hexagonal structure with $a = 7.0$ and $c = 11.1 \text{ \AA}$ for solid phase II (stable below 82K). Kleinman *et al.* (8) found similar results. Recently, because magnetic studies (6) indicated complete absence of solid phase I in the deuterated compound $\text{Li}(\text{ND}_3)_4$, we were led to reevaluate the X-ray diffraction data on $\text{Li}(\text{NH}_3)_4$ and existing neutron diffraction data (9) on $\text{Li}(\text{NH}_3)_4$ and $\text{Li}(\text{ND}_3)_4$. The X-ray reflections observed at 77K are better indexed as a single body-centered cubic phase (10). Solid phase II of $\text{Li}(\text{NH}_3)_4$, stable below 82K, appears to belong to space group $I\bar{4}3d$, $a = 14.93 \text{ \AA}$, with 16 lithium atoms and 16 nitrogen atoms on Wyckoff position c and 48 nitrogens on Wyckoff position e . The same structure holds for $\text{Li}(\text{ND}_3)_4$. Below 25K, extra reflections appear, corresponding to formation of a superstructure with period $2a$; this is coincident with onset of antiferromagnetic ordering below this temperature.

Granted that $\text{Li}(\text{NH}_3)_4$ can be regarded as

lithium metal which has been expanded by insertion of NH_3 so that Li-Li has gone from 3 to 6 \AA , a relevant question is: At what separation would we expect a metal-nonmetal transition to occur? In the Hubbard (11) model (Fig. 1), as one-electron centers are progressively brought together, the energy gap U , between having only one electron on each center and having two electrons on the same site, progressively shrinks as the bandwidth B , due to overlap of wave functions, widens. The transition from the insulating regime to the metallic regime is supposed to occur at $U/B = 1.15$, where the upper Hubbard band overlaps the lower and there is no activation energy for electron transport. Mott, however, has argued that the nonmetal-to-metal transition should be discontinuous due to cooperative loosening of all the electrons by a sudden fall in the screened potential. Mott (12) predicted that the $M-NM$ transition should occur at a critical electron concentration, n_c , given by $n_c^{1/3} a_H \approx 0.25$, where a_H is an effective hydrogenic radius for the isolated metal atom in the low-electron density limit, i.e., in the nonmetallic regime far from the transition. An extensive analysis of experimental data (13), spanning

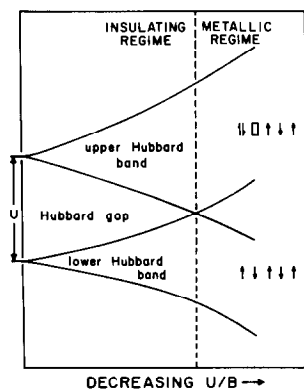


FIG. 1. Hubbard model for the metal-nonmetal transition. The metal-nonmetal transition occurs when the upper and lower Hubbard bands overlap. U is the electron-electron repulsion energy for two electrons on the same site; B is the bandwidth.

doped semiconductors, nonstoichiometric bronzes, and argon-trapped metal dispersions, has indeed shown that the experimental criterion for the metal–nonmetal transition is $n_c^{1/3} a_H^* = 0.26 \pm 0.03$, where a_H^* is now characteristic of a realistic wave function for the isolated species. For Li-NH_3 , n_c is $9.94 \times 10^{20} \text{ cm}^{-3}$ and a_H^* is 2.76 \AA . $\text{Li(NH}_3)_4$ has 4.8×10^{21} Li atoms per cubic centimeter and apparently, from the physical properties, lies clearly on the metallic side of the M – NM transition. It was therefore of interest to investigate the analogous methylamine compound, as the extra bulk of the methyl group in $\text{Li(CH}_3\text{NH}_2)_4$ would presumably expand the lithium–lithium separation and perhaps push it over to the nonmetallic side of the M – NM transition. Although the existence of compound $\text{Li(CH}_3\text{NH}_2)_4$ has not been unequivocally established, we report here on a comparative study of lithium in ammonia, in methylamine, and in [2.1.1] cryptate. The indication is that the metal–nonmetal transition is straddled by these three systems.

Experimental

Starting materials were 99.99% lithium from Lithium Corporation of America, 99.99% ammonia from Matheson, and 98% methylamine from Matheson. Impurities in the methylamine, as checked by mass spectrometry, were 0.0% ammonia, 0.8% (max) dimethylamine, 0.6% (max) trimethylamine, and 0.8% (max) water. The cryptand purification and preparation have been described elsewhere (14). Magnetic susceptibilities were measured by the Faraday method in sealed Spectrosil buckets using standard techniques previously employed (15). One special feature was *in situ* correction for sample bucket and core diamagnetism by warming samples to room temperature to destroy free electrons and hence free electron susceptibility.

Results and Discussion

Figure 2 summarizes the descriptions of the phenomenological models that apply in the lithium–ammonia system as the concentration of lithium is progressively increased. In the most dilute solutions ($<10^{-3}$ MPM), behavior is electrolytic with solvated lithium cations and solvated electron anions. The electrons are trapped in cavities formed by the ammonia dipoles and there is a large energy difference between one electron per cavity (designated D_1^0 in the figure) and two electrons paired in the same cavity (D_1^-). The Fermi energy lies between these two energies. As the Li/NH_3 concentration is raised to the range 10^{-3} to 10^{-1} MPM, cluster states appear, probably consisting of several cavities bridged by Li^+ cations. Again there is a considerable gap in energy between the $1e^-$ -per-cavity states

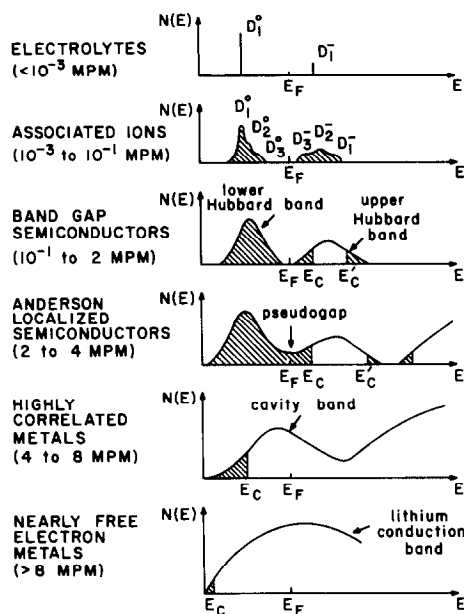


FIG. 2. Metal–nonmetal transition in lithium–ammonia solutions. $N(E)$ is the density of states at energy E . As the concentration of lithium is increased, from top to bottom in figure, the position of the Fermi level E_F changes from localized to delocalized regimes. Shaded areas represent localized states. E_c is the mobility edge.

(D_1^0 , D_2^0 , D_3^0) and the doubly occupied cavities (D_3^- , D_2^- , D_1^-). On further increase of lithium concentration, to the range 10^{-1} to 2 MPM, broad Hubbard bands appear as cavity wavefunctions in individual cavities begin to overlap. States are extended but low in mobility (shaded areas in the figure), so conductivity is still limited. Disorder both in spatial separation between cavities and in trapping energies leads to Anderson (16) localization between 2 and 4 MPM. In the range 4 to 8 MPM metallic behavior begins to appear but in subdued fashion as the electrons are believed to be confined to cavity-wavefunction-generated states. Only when concentrations of lithium exceed about 8 MPM is it believed that the conduction band takes on Li 3s character as the Li 3s energies fall below those of the cavity-dominated wavefunctions. Behavior is nearly free electronic in that the magnetic susceptibility is temperature-independent Pauli and the Hall voltage is almost that expected of a nearly free electron metal.

The concentrations chosen to divide the various electronic regimes proposed are somewhat arbitrary. They are expected to vary with temperature since the band structure of a liquid is a strong function of temperature. At 220K changes in various properties are observed at the concentrations chosen. Near 10^{-3} MPM, a drop in the equivalent conductance (17) is observed, suggesting that the solvated metal cation and the electron are no longer independent of each other. It is thought that the diamagnetic susceptibility (18) observed between 10^{-3} and 2 MPM is due to antiferromagnetic ordering of the cavity-trapped electrons. Near 10^{-1} MPM, the equivalent conductance begins to rise again, suggesting the onset of electronic conduction via the excitation of electrons across the Hubbard gap. Above 2 MPM, the electronic susceptibility reaches positive values, indicating a finite density of states due to the overlap of the Hubbard bands. Since the

conductivity remains below Mott's criterion for a minimum metallic conductivity of $\sim 100 \Omega^{-1} \text{ cm}^{-1}$ (19), it is assumed that the electrons are localized by disorder.

The transition to the metallic state is taken to be 4 MPM, as this is the Li concentration at the critical point for liquid-liquid phase separation. It has been suggested that the phase separation is a symptom of the metal-nonmetal transition (20). The conductivity increases with temperature due to a decrease in the density of states (as is typical for liquids) (21) and not because there is an energy of activation for transport. The solutions have the blue color characteristic of the cavity transition till near 8 MPM and conduction must therefore occur in a narrow band formed by overlap of the cavity wavefunctions. Above 8 MPM, the solutions are bronze and have properties predicted by the nearly free electron picture. Liquid $\text{Li}(\text{NH}_3)_4$ seems to be close to an ideal metal.

What happens to $\text{Li}(\text{NH}_3)_4$ as the temperature is lowered? Upon freezing, the nearly free electron properties seem to be retained. The resistivity drops by the expected liquid-to-solid factor due to a density change (about 5) and the Hall voltage and susceptibility rest free electronic. Figure 3A shows the expected situation in the range 82–89K. Behavior is nearly free electronic. In Fig. 3B, for the range 25–82K, the cavity bands are seen to have dropped in energy below the lithium levels, probably because of a minor crystallographic distortion within the cubic system. Behavior now is no longer nearly free electronic but more like that of a highly correlated metal (susceptibility is Curie-Weiss temperature-dependent and the Hall voltage has significantly increased). In Fig. 3C, corresponding to the situation below $\sim 25\text{K}$, upper and lower Hubbard bands appear with a pseudogap at the Fermi level, apparently due to further lattice distortion that goes with the antiferromagnetic superlat-

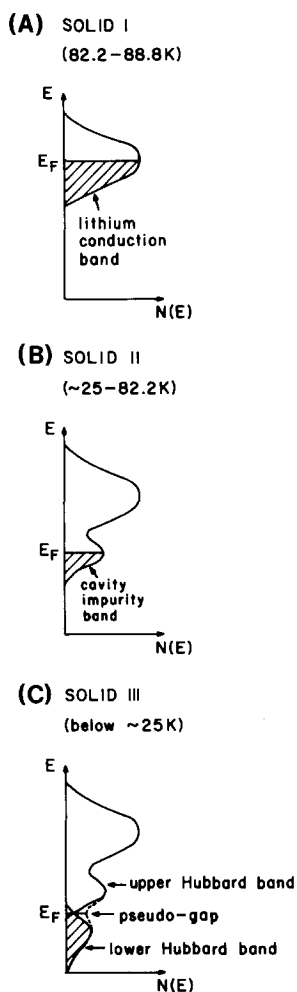


FIG. 3. Proposed band structures of solid $\text{Li}(\text{NH}_3)_4$. (A) Phase I is a nearly free electron metal with a half-filled conduction band based on lithium orbitals. (B) Phase II is a highly correlated metal with a half-filled cavity-based band. (C) Phase III has a pseudogap in the density of states at the Fermi level. Shading designates filled states.

tice formation. By this stage $\text{Li}(\text{NH}_3)_4$, though still metallic, seems to have lost many of its free electron properties.

What happens when we replace ammonia by methylamine? Although the original motivation for its investigation was simply to add more bulk (via the methyl group) between the lithium atoms, there is a concomitant decrease in the dielectric constant. Al-

though the effective dielectric constant, from the weighted average of optical and static values, drops only from 5.22 to 4.90, the effect is to shrink the electron-trapping cavity and increase the expected critical density for metallization from 9.94×10^{20} to $18.5 \times 10^{20} e^-/\text{cm}^3$. This can be easily deduced from the Mott criterion $n_c^{1/3} a_H^* = 0.26$. Consequently, the nonmetal-to-metal change in lithium–methylamine should be deferred to considerably higher concentration (12–16 MPM, rather than 4–8 MPM as in lithium–ammonia) and at all concentrations the free electron properties should be less evident.

Figure 4 shows schematically the sequence of phenomenological models believed to hold for the lithium–methylamine system. Because the electron cavity is smaller and deeper, double-electron occupancy of a cavity is energetically less favorable. (Note the bigger energy spacing between D_1^0 and D_1^- in Fig. 4.) The Hubbard bands are farther apart, they close less rapidly, and the pseudogap persists to higher concentration. Even the most concentrated solutions (>15 MPM) are blue and the electrons are probably still in cavity states.

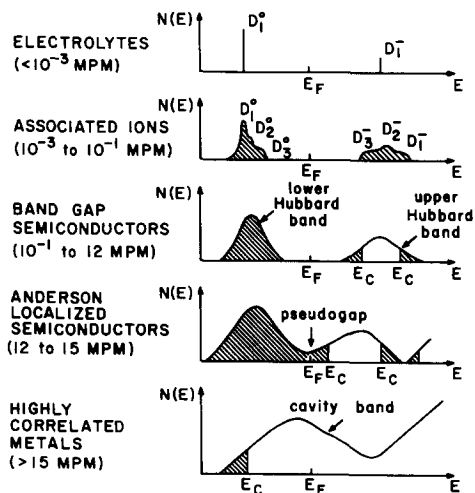


FIG. 4. Metal–nonmetal transition in lithium–methylamine solutions. Symbols are as in Fig. 2.

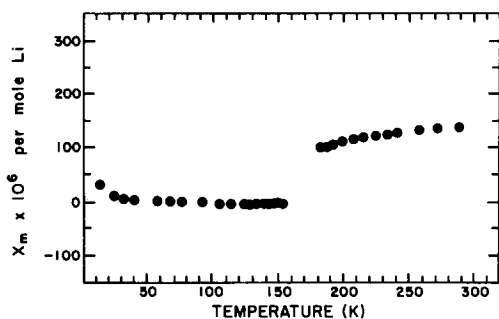


FIG. 5. Magnetic susceptibility as a function of temperature for 22 mole% lithium in methylamine. This is the free electron susceptibility after *in situ* correction for diamagnetic cores and sample container. Uncertainty is about the size of the dots.

Although ESR (22) and conductivity (23) measurements suggest that liquid $\text{Li}(\text{CH}_3\text{NH}_2)_4$ is metallic, the $\text{Li}-\text{CH}_3\text{NH}_2$ system never reaches the nearly free electron behavior as is found in concentrated $\text{Li}-\text{NH}_3$. The behavior remains that of a highly correlated metal.

Indeed, as is seen in Fig. 5, which shows the magnetic susceptibility of a concentrated lithium-methylamine solution as a function of temperature, the free electron susceptibility, i.e., after correction for diamagnetism, goes to zero for the solid

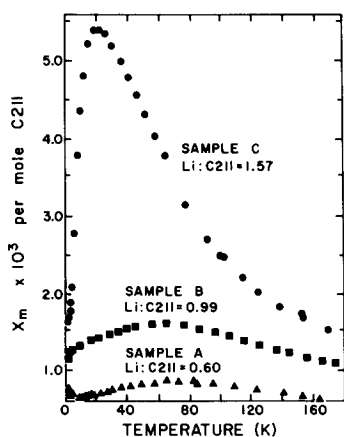


FIG. 6. Magnetic susceptibility as a function of temperature for various mixtures of lithium and [2.1.1] cryptand. The values have been corrected for diamagnetic cores and container.

$\text{Li}(\text{CH}_3\text{NH}_2)_4$ below 155K. Local electron pairing seems to dominate the behavior and this solid appears to be a semiconductor with a finite Hubbard energy gap.

The extreme of the above shows up in the lithium cryptate electrides. As described elsewhere (5), the lithium cation is trapped inside the cryptand cage and the electron is squeezed out and forced to find a home in some external interstitial cavity between the cryptand moieties. The electrons, localized and unpaired, exert their full magnetic moment. As shown in Fig. 6, the magnetic susceptibility is large and, at higher temperatures, classically paramagnetic. The moment per lithium is 1.7 BM for both $\text{Li}:\text{C211} = 0.6$ and $\text{Li}:\text{C211} = 0.99$. Only when there is a large excess of Li (Sample C in Fig. 6 with $\text{Li}:\text{C211} = 1.57$) does the moment fall below the expected $S = \frac{1}{2}$ value to 1.2 BM. (This depression of the moment with excess Li is probably due to pairing of electrons in two separate cavities joined by an intervening Li^+ , which effectively gives the equivalent of an Li^- anion.)

The main points to note in Fig. 6 are that the molar electron susceptibilities are more than two orders of magnitude greater than those for $\text{Li}:\text{NH}_3$ and $\text{Li}:\text{CH}_3\text{NH}_2$; also, they decrease markedly at very low temperatures. The low-temperature decrease is not a normal antiferromagnetism but appears to be fitted by a local pairing law involving adjacent electrons.

Table I summarizes the comparison of the various lithium regimes extending from pure lithium metal through progressive dilution first by ammonia, then by methylamine, and finally by [2.1.1] cryptand. It is evident that $\text{Li}(\text{NH}_3)_4$ lies on the metallic side of the metal-nonmetal transition, but becomes "less metallic" as the temperature is lowered. $\text{Li}(\text{CH}_3\text{NH}_2)_4$, on the other hand, appears to be right at the transition and, in fact, goes from "metallic" to "non-metallic" as the temperature is lowered. The cryptand LiC211 is clearly nonmetallic.

TABLE I
SUMMARY OF MAGNETIC AND ELECTRIC BEHAVIOR
IN VARIOUS LITHIUM SYSTEMS

System	$\chi_m \times 10^6$ per mole Li	σ ($\Omega^{-1} \text{ cm}^{-1}$)	Electronic regime
Li metal	+14.2 (200K)	$>10^6$ ($\sim 100\text{K}$)	Free electron metal
Li(NH ₃) ₄ Liquid	+60 (88.8K)	$\sim 1.2 \times 10^4$ ($\sim 90\text{K}$)	Nearly free electron metal
Solid I	+56 (85K)	$\sim 7.0 \times 10^4$ ($\sim 85\text{K}$)	Nearly free electron metal
Solid II	+36 (80K)	$\sim 5.6 \times 10^4$ ($\sim 80\text{K}$)	Highly correlated metal
Solid III	+49 (25K)	—	Highly correlated metal
Li(CH ₃ NH ₂) ₄ Liquid	+96.4 (155K)	$\sim 4 \times 10^2$ (200K)	Highly correlated metal
Solid	-9.4 (155K)	—	Small band gap semi conductor
Li-C211	+1000 (200K)	$<10^{-2}$	Large band gap semi conductor

Note. The materials above the dashed line are metals and those below are insulators.

As a final point, it is interesting to speculate on the probable effect of pressure on these materials. At first sight, it might appear that a rise in pressure should reduce the average spacing between lithium centers and therefore, in the Mott sense, increase metallic behavior. However, this ignores the effect of the dielectric host, in particular the effect it has on the size of the electron-trapping cavity. It is now conjectured that an increase in pressure will deepen the potential well in which the electron is trapped and decrease the radial spread of the wavefunction. If this is indeed the case, as the pressure is increased the energy bands in the cavity-centered conduction regime would narrow and begin to open a gap between Hubbard bands. Solid

phase III of Li(NH₃)₄ already appears to fit this description, and low-temperature Li(NH₃)₄ might become an insulator with increasing pressure. However, for solid phase I of Li(NH₃)₄, in which conduction is presumably based on Li 3s orbitals, increased pressure should decrease the density of states and make the material a better conductor. Experiments to test these predictions are now in progress.

Acknowledgments

We would like to thank the National Science Foundation for sponsoring this research through Grant DMR 81-20324 and the AFOSR and the Materials Science Center at Cornell University for providing subsidiary support. P. P. Edwards wishes to acknowledge the support of the Science Research and Engineering Council (U.K.). We are also specially grateful to Professor J. L. Dye and J. S. Landers of Michigan State University for collaborating on the lithium-cryptand studies and to David C. Johnson of Cornell University for important help in the sample preparations. Enlightening discussions with Dr. Martin Harrison and Dr. B. K. Chakraverty have been deeply appreciated.

References

1. For a review, see J. C. THOMPSON, "Electrons in Liquid Ammonia," Oxford Univ. Press (Clarendon), London/New York (1976).
2. L. V. COULTER, S. H. LEE-BECHTOLD, AND V. MADHVARAJA, *J. Chem. Thermodyn.* **13**, 815 (1981).
3. M. D. ROSENTHAL AND B. W. MAXFIELD, *J. Solid State Chem.* **7**, 109 (1973); R. C. CATE AND J. C. THOMPSON, *J. Phys. Chem. Solids* **32**, 443 (1971); J. A. MORGAN, R. L. SCHROEDER, AND J. C. THOMPSON, *J. Chem. Phys.* **43**, 4494 (1965).
4. W. S. GLAUNSINGER, S. ZOLOTOV, AND M. J. SIENKO, *J. Chem. Phys.* **56**, 4756 (1972).
5. J. S. LANDERS, J. L. DYE, A. STACY, AND M. J. SIENKO, *J. Phys. Chem.* **85**, 1096 (1981).
6. A. M. STACY, D. C. JOHNSON, AND M. J. SIENKO, *J. Chem. Phys.* **76**, 4248 (1982).
7. N. MAMMANO AND M. J. SIENKO, *J. Amer. Chem. Soc.* **90**, 6322 (1968).
8. L. KLEINMAN, S. B. HYDER, C. M. THOMPSON, AND J. C. THOMPSON, in "IUPAC: Metal-Ammonia Solutions" (J. J. Lagowski and M. J. Sienko, Eds.), p. 229, Colloque Weyl II, Ithaca, N.Y. (1969).

9. P. CHIEUX, M. J. SIENKO, AND F. DEBAECKER, *J. Phys. Chem.* **79**, 2996 (1975).
10. A. M. STACY AND M. J. SIENKO, *Inorg. Chem.* **21**, 2294 (1982).
11. J. HUBBARD, *Proc. Roy. Soc. London Ser. A* **276**, 238 (1963); **277**, 237 (1964); **281**, 401 (1964).
12. N. F. MOTT, *Proc. Phys. Soc. London Sect. A* **62**, 416 (1949); *Canad. J. Phys.* **34**, 1356 (1956); *Philos. Mag.* **6**, 287 (1961).
13. P. P. EDWARDS AND M. J. SIENKO, *Phys. Rev. B* **17**, 2575 (1978).
14. J. L. DYE, *J. Phys. Chem.* **84**, 1084 (1980).
15. J. E. YOUNG, JR., Ph.D. thesis, Cornell University (1971).
16. P. W. ANDERSON, *Phys. Rev.* **109**, 1492 (1958).
17. Ref. (3), p. 79.
18. A. DEPRIESTER, J. FACKEURE, AND J. P. LELIEUR, *J. Phys. Chem.* **85**, 272 (1981).
19. N. F. MOTT, "Metal-Insulator Transitions," Taylor & Francis, London (1974).
20. P. P. EDWARDS AND M. J. SIENKO, *J. Amer. Chem. Soc.* **103**, 2967 (1981).
21. M. CUTLER, "Liquid Semiconductors," Academic Press, New York (1977).
22. P. P. EDWARDS, J. R. BUNTAINE, AND M. J. SIENKO, *Phys. Rev. B* **19**, 5835 (1979).
23. R. HAGEDORN AND M. J. SIENKO, *J. Phys. Chem.* **86**, 2094 (1982).